



The Society shall not be responsible for statements or opinions advanced in papers or in discussion at meetings of the Society or of its Divisions or Sections, or printed in its publications. Discussion is printed only if the paper is published in an ASME Journal. Papers are available from ASME for fifteen months after the meeting.
Printed in USA.

Copyright © 1990 by ASME

The Development of Axial Turbine Leakage Loss for Two Profiled Tip Geometries Using Linear Cascade Data

JEFFREY P BINDON
and
GEORGE MORPHIS
University of Natal
Durban
South Africa

Abstract

To assess the possibility of tip clearance loss reduction and to explore the nature and origin of tip clearance loss, blade tip geometries which reduce the roughly 40% of total loss occurring within the gap were studied. The shapes investigated aimed at reducing or avoiding the gap separation bubble thought to contribute significantly to both internal gap loss and to the endwall mixing loss. It was found that radiusing and contouring the blade at gap inlet eliminated the separation bubble and reduced the internal gap loss but created a higher mixing loss to give almost unchanged overall loss coefficients when compared with the simple

sharp edged flat tipped blade. The separation bubble does not therefore appear to influence the mixing loss. Using a method of assessing linear cascade experimental data as though it were a rotor with work transfer, one radiused geometry, contoured to shed radial flow into the gap and reduce the leakage mass flow, was found to have a significantly higher efficiency. This demonstrates the effectiveness of the data analysis method and that cascade loss coefficient alone or gap discharge coefficient cannot be used to accurately evaluate tip clearance performance. Contouring may ultimately lead to better rotor blade performances.

Nomenclature

C_v	= velocity ratio V/W	V_θ	= swirl velocity
\bar{C}_L	= loss coefficient	W	= relative velocity
C_m	= mixing loss coefficient	w	= specific work
C_g	= internal gap loss coefficient	Z	= spanwise flow integration height
C_w	= work coefficient = $\rho \bar{w} / \frac{1}{2} \rho W^2$	z	= spanwise distance
C_D	= gap discharge coefficient = \dot{m} / \dot{m}_{r_s}	β	= relative flow angle
C_f	= gap mass flow coefficient = gap mass flow / inlet flow through 1 pitch x blade length of 1/4 chord	ρ	= density
C'_L	= 1D gap loss coeff at given chord position	η	= efficiency
\dot{m}	= mass flow	Subscript notation	
p	= pressure	o	= total quantity
S	= pitch	1	= cascade inlet
s	= pitchwise distance	2	= cascade exit
U	= hypothetical rotor velocity	ts	= total to static
V	= absolute velocity	tt	= total to total
V_{2ia}	= mass averaged vel above vortex at height Z_2	is	= isentropic or loss free
		x	= axial

1 Introduction

In this paper the tip clearance loss is measured in a linear cascade for 3 different gap geometries with the threefold objective of improving the understanding of the flow phenomena giving rise to rotor loss, of developing an experimental procedure to assess rotor efficiency based on detailed stationary cascade anemometry and of identifying tip shapes for improved performance.

With respect to the flow phenomena responsible for tip clearance loss, Bindon (1988) showed that for a simple sharp edged flat tipped blade, the loss generated internally within the gap was 40% of the overall tip region loss while 50% was due to the mixing of leakage vortex over the final half of the cascade flow. It appeared that chordwise flow inside the gap separation bubble caused not only the high internal gap loss but was also the reason for a low discharge coefficient. Over the forward half of the blade, leakage flow reattaches behind the bubble with a relatively low loss and high discharge coefficient.

At mid chord however where the gap pressure is the lowest, well below that at gap exit on the suction side, the flow inside the bubble accumulates and is ejected from the gap by mixing with the high velocity inlet jet induced by the low pressure at that point. Thus high internal gap loss and low discharge coefficient develops at mid chord and a concentration of low momentum fluid is fed into the suction corner flow at this point. Since this flow encounters the diffusing gradient of the suction corner, it was suggested that it may "separate" to form the high mixing loss seen to develop after mid chord. No mixing loss was seen on the endwall prior to the 50% chord position despite significant leakage occurring over the forward half of the blade.

Thus the formation of both the internal gap loss and the mixing loss is thought to be related to the separation bubble.

In order to improve the understanding of the loss phenomena as well as to address the objective of developing improved gap shapes, it was considered profitable to examine tip geometries which avoid the formation of the bubble. In a preliminary study, Morphis and Bindon (1988), showed that a radiused edge eliminated the separation bubble and the associated very low gap inlet static pressures. The first tip geometry chosen was therefore the simple flat tip with radiused edge. The second shape was a contoured tip intended to avoid the separation bubble and to shed radial flow into the gap so as to reduce the leakage mass flow.

An experimental technique is required to compare the performance of the different gap geometries. While the ultimate test is that on an actual rotor, as done by for example by Offenburg et al (1987) and Booth et al (1982), such a test does not normally provide any flow detail since rotor flow anemometry is costly. Booth et al (1982) approached the problem by measuring the overall gap discharge coefficient in gap simulation rigs. This method provides no flow detail and is based on the assumption that discharge coefficient is the dominant factor. Bindon (1987), (1988), used the total pressure loss coefficient obtained in a linear cascade with tip clearance. While this provides flow detail, in reality rotor performance depends on the Euler work obtained by flow deflection. Total pressure loss, while having an important effect,

is not the only factor involved in determining rotor work transfer. As shown in Figure 1, loss will reduce the velocity but ultimately it is the change in angular momentum that creates rotor output. This paper therefore presents and uses an analysis of experimental cascade data whereby the stationary velocity vectors are converted to the rotating frame by the addition of a hypothetical blade speed to evaluate a hypothetical rotor work and efficiency.

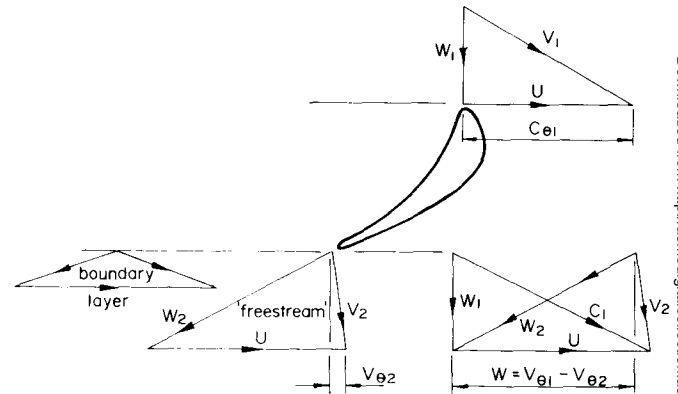


Figure 1

By adding blade speed U to inlet velocity W and outlet velocity W a stationary cascade flow field is converted to a simulated rotor with absolute velocities V_1 and V_2

2 Rotor performance simulation

The performance of a stationary cascade may be gauged by determining the loss in total pressure. Such a loss (or entropy increase) should be used with caution as a performance indicator for a rotor where the work output is created by the change in swirl velocity. Thus the effect of both flow deflection and pressure loss in the presence of tip clearance needs to be included in a comparative performance assessment. Since flow field measurements are easier to make in stationary cascades than in moving rotors, cascade flow field data is not only more accessible but also provides more intricate flow detail which enhances the understanding of the flow physics.

If therefore stationary flow field data could be adapted to simulate a rotor flow, a tool for the evaluation of secondary flow phenomena in rotors would become available which is both inexpensive and highly informative. The proposed adaptation of linear cascade data is shown in Figure 1 where the blade speed U is added to the measured cascade velocities W_1 and W_2 at inlet and outlet to create a simulated rotor with absolute velocities V_1 and V_2 and work transfer w . The intention of this section is to obtain the mean work transfer \bar{w} for the whole measured flow field and use it to deduce a simulated rotor efficiency.

The incompressible energy equation for a rotor with work transfer is :-

$$p_{c1} = p_2 + \frac{1}{2} \rho \bar{V}_2^2 + \Delta \bar{p} + \rho \bar{w} \quad \text{-----(1)}$$

The terms are all mass averaged quantities which are determined by integration of the whole flow field.

In an incompressible rotor the pressure difference represents the isentropic change. Therefore rotor efficiencies may be defined in various ways following the normal concept of real and ideal work. Thus :-

$$\eta = w/w_{is} = \rho \bar{w} / \Delta p \quad \text{-----(2)}$$

where Δp is the driving pressure difference.

For the "total to total" case :-

$$\eta_{tt} = \frac{\rho \bar{w}}{p_{o1} - p_{o2}} = \frac{\rho \bar{w}}{\rho \bar{w} + \Delta p_o} \quad \text{-----(3)}$$

The "total to static" case is

$$\eta_{ts} = \frac{\rho \bar{w}}{p_{o1} - p_2} = \frac{\rho \bar{w}}{\rho \bar{w} + \Delta p_o + \frac{1}{2} \rho \bar{V}_2^2} \quad \text{-----(4)}$$

When applied to the simulated "rotor" some explanations and assumptions are needed. The kinetic energy is simply the mass averaged integration of V_2 . The work term is the Euler work $U(V_{\theta 1} - V_{\theta 2})$ mass averaged over the inlet and outlet flows. The total pressure loss term, because it primarily involves fluid friction generated in the flow over the blade and endwall surfaces and that generated by secondary flows, is assumed to be the same for the stationary cascade and for the "rotor". The main factor that would make the two losses different in reality would relate to the different outer endwall motion (for unshrouded blades) which affects the shear forces, the leakage flow quantity and sets up the "scraping vortex".

Non dimensionalising each term with the cascade inlet freestream velocity head $\frac{1}{2} \rho W^2$

$$\eta_{tt} = C_w / (C_w + \bar{C}_L) = 1 / (1 + \bar{C}_L / C_w) \quad \text{-----(5)}$$

$$\eta_{ts} = C_w / (C_w + \bar{C}_L + C_{V_2}^2) = 1 / (1 + \bar{C}_L / C_w + C_{V_2}^2 / C_w) \quad \text{-----(6)}$$

The integration for the rotor work transfer coefficient C_w would normally span the whole of the rotor passage between hub and tip. Since the resulting efficiency would then be somewhat insensitive to changes in tip clearance performance because of the large loss free zones at mid height, only the endwall zone affected by leakage is integrated. In Bindon (1988) the reference mass flow was that of free inlet fluid through an area 1 pitch x a spanwise distance of 1/4 chord, a figure selected as providing a height greater than the affected zone at cascade exit. This reference mass flow is retained here.

At cascade exit, the integration is taken up to a height Z_2 just sufficient for the mass flow through the exit plane to match the mass flow through the inlet plane. The exit plane height will depend on the extent and intensity of the secondary flow and also of the flow direction and is found by iteration, for each tip clearance shape and associated flow field, from :-

$$\dot{m} = \rho W S Z_1 = \int_0^S \int_0^{Z_2} \rho W_2 \cos \beta_2 dz ds$$

For convenience, this can be non dimensionalised with the mass flow \dot{m}

$$1 = \int_0^S \int_0^{Z_2} \frac{W_2}{W} \cos \beta_2 \frac{dz ds}{Z_1 S} \quad \text{-----(7)}$$

The work term $\rho \bar{w}$, and later the work coefficient C_w , can be found by mass averaging the Euler work $U(V_{\theta 1} - V_{\theta 2})$ for the inlet and outlet flow fields.

$$\bar{w} = \frac{\int \dot{m} U V_{\theta 1} d\dot{m}}{\dot{m}} - \frac{\int \dot{m} U V_{\theta 2} d\dot{m}}{\dot{m}} \quad \text{-----(8)}$$

As shown in Figure 1 for this hypothetical rotor analysis of flow in the leakage affected zone near the tip, the linear cascade had an "axial" inlet and thus the simulated swirl velocity $V_{\theta 1}$, is constant even within the inlet boundary layer.

$$\begin{aligned} C_w &= \frac{\rho \bar{w}}{\frac{1}{2} \rho W^2} = \frac{\rho}{\frac{1}{2} \rho W^2} \left(\frac{\int U V_{\theta 1} d\dot{m}}{\dot{m}} - \frac{\int U V_{\theta 2} d\dot{m}}{\dot{m}} \right) \\ &= \frac{2}{W^2} \left(\frac{U^2 \int d\dot{m}}{\dot{m}} - \frac{U \int_0^S \int_0^{Z_2} V_{\theta 2} \rho W_2 \cos \beta_2 dz ds}{\rho W S Z_1} \right) \\ &= \frac{2U^2}{W^2} - \frac{U}{W} \int_0^S \int_0^{Z_2} \frac{V_{\theta 2}}{W} \frac{W_2}{W} \cos \beta_2 \frac{dz ds}{Z_1 S} \quad \text{-----(9)} \end{aligned}$$

3 Cascade geometry and apparatus

A linear cascade of seven 186 mm span, 186 mm chord blades with the same profile and spacing as in Bindon (1988) were used. As shown in Figure 2, three tip shapes were used, a flat sharp edged reference blade which corresponded with the previous study and two rounded tip designs to minimise the size and formation of the separation bubble in the gap. The first rounded tip has a rounded pressure side edge with a radius of 2.5 gap widths as found by Morphis and Bindon (1988) to avoid bubble formation. The second tip is intended to deflect flow radially into the gap so as to reduce the gapwise component and hence the leakage mass flow. The contours used to turn the flow radially are generously curved to control the bubble formation. All results are for a gap size of 2.5% chord. In all the results the cascade exit Reynolds Number was 470 000.

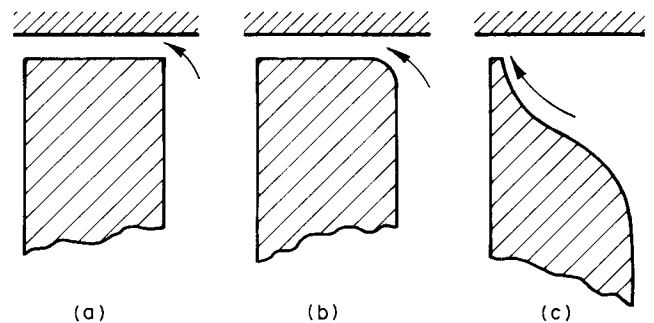


Figure 2
Schematic of the three blade tip shapes tested
a) Square tip with sharp pressure edge
b) Flat tip with radiused pressure edge
c) Contoured tip radiused to create radial leakage flow

A five hole probe survey was done in the cascade exit plane using a combination of two separate traverses. The first traverse was done with a 1.5mm x .5mm 3 hole cobra probe with the stem shaped in a tight gooseneck. This allowed access to the flow through holes in the tunnel wall and allowed the main pitchwise flow direction to be determined by null yawing without probe tip movement. The second traverse was done with a 1.8mm x .9mm two hole probe that was manually yawed in the main pitchwise flow direction as determined by the first traverse. The two holes were orientated in the radial direction to provide the radial flow components.

As described by Bindon (1988), the total secondary flow and leakage mixing loss is found by subtracting the loss occurring within the clearance gap from the total loss measured in the cascade exit plane. The internal gap loss was found from 10 endwall traverses of the gap exit flow with the gooseneck probe located exactly in line with the suction surface. For the two flat tipped gap geometries there will be no radial components. For the contoured tip specifically chosen to create radial flow, the regime was too narrow to use the second probe. Fortunately the resulting inaccuracy is not serious since the cobra probe alone would tend to overestimate the total pressure loss and, as will be discussed later, the loss was found to be relatively low.

4 Experimental results

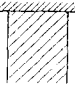
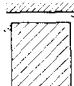


Table 1 presents the experimental results for the 3 tip geometries as well as for the zero clearance case necessary for comparison and to provide some data to determine the mixing loss. Some quantities in the table are defined in Section 2. All the results were computed for an inlet to blade speed ratio W/U of 1/2 .

5 Internal Gap Loss and Leakage Mixing Loss.

The losses formed within the gap have been shown to be an important part of the overall loss in a cascade with tip clearance. As with any other loss measurement, the gap loss should be determined from traverses at inlet and outlet. However the flow at the gap inlet has intense directional changes within the space of a few millimeters and is difficult to traverse.

Since the inlet loss is largely contained in the boundary layer against the endwall, the contoured blade tip geometry presents the possibility of determining

Table 1
Tip Region Performance Criteria for Various Tip Clearance Geometries. (clearance = 2.5% chord)

Schematic of Geometry					
Rotor eff ts	η_{ts}	97.70	76.90	74.09	80.68
Rotor eff tt	η_{tt}	98.38	87.81	86.56	88.82
Loss coefficient	\bar{C}_L	0.152	0.874	0.964	0.843
Internal gap loss	C_g	-	0.270	0.061	0.062
Mixing loss	C_m	0.152	0.452	0.751	0.629
Gap exit normal ke		-	0.684	0.926	0.869
Work Coef	C_w	9.225	7.869	6.212	6.700
Exit Height	Z_2	1.046	1.123	1.112	1.179
Gap Mass Flow Coef	C_F	-	0.240	0.287	0.256
Gap discharge Coef	C_D	-	0.824	0.926	0.920
Vel Coef	$(\bar{V}_2/W)^2$	1.194	1.862	1.994	1.600

both the gap inlet and gap exit loss from a single traverse at gap exit. All of these traverses showed a virtually loss free core flow which separates the inlet loss against the endwall and the loss in the boundary layer against the blade. The loss on the endwall does not have a chance to grow because the flow path length is short and the pressure gradient accelerating. Since the gap inlet loss is due to the cascade inlet boundary layer and endwall shear flow being drawn into the gap, the variation of this ingested loss quantity between the three tip geometries should not be large and the value measured for the contoured blade (0.037) was assumed to apply to the other two tip shapes.

The internal gap loss coefficients are also presented in Table 1 above and figures for the radiused blade and for the contoured tip are only 22% of that for the sharp edged square tip thus confirming that the separation bubble is largely responsible for the formation of internal gap loss and can be significantly reduced by suitable contouring.

Figure 3 shows the variation of gap loss with chord for the sharp edged blade. The shape of the curve is very different from that presented in Bindon (1988) for the same blade profile and tip region geometry. A peak had previously been seen at mid chord. The total integrated loss for the gap flow is lower at 31% of total as compared to the previously measured 38%. This difference in the distribution of loss between the leading and trailing edges for the same blade shape but made in different laboratories and tested in different wind tunnels would indicate that the microflow phenomena measured in tip gaps are highly sensitive, not easily reproduced and the applicability to completely different profiles is doubtful.

The sharp peak previously seen in the gap loss distribution had been linked with the flow within the bubble accumulating near mid chord where the static

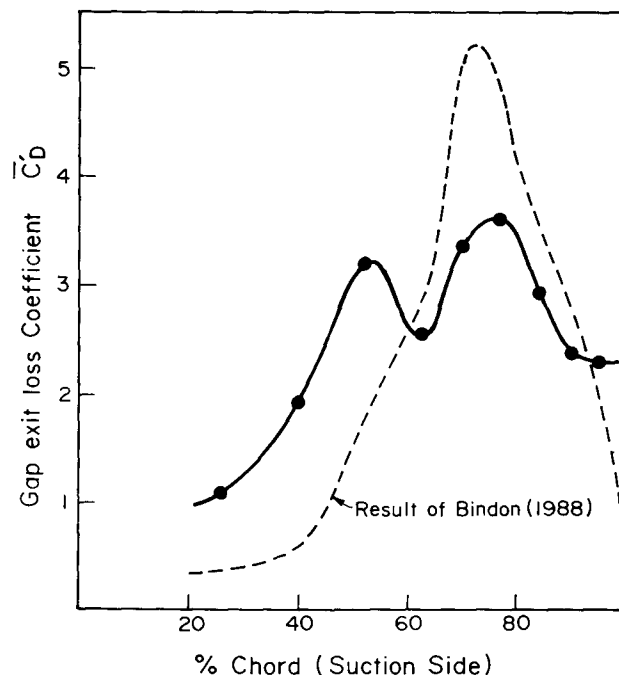


Figure 3
Distribution of internal clearance gap loss with chord. Square sharp edged blade with clearance of 2.5% chord.

pressure was a minimum. The loss peak was thought to result from the high velocity leakage jet mixing with the bubble fluid. The absence of such a peak in the present study suggests that there is a more even mixing of the bubble fluid across the length of the blade chord. Despite the lower internal gap loss measured in the present study, the overall cascade loss was the same as that previously measured.

As in Bindon (1988) the mixing loss is calculated by subtracting the internal gap loss and the endwall shear flow and secondary loss from the overall cascade loss. It is assumed that the normal secondary flow loss is that found for the zero clearance case. The results appear in Table 1. The figure of 0.451 for the flat sharp edged reference blade compares favourably with that of 0.4 measured previously.

The highest value is for the radiused edge and the lowest for the square tip. The hypothesis suggested in Bindon (1988) that the mixing loss could possibly be due to the separation of the high loss wake within the leakage flow leaving the gap is not corroborated because in both the cases where the separation bubble has been eliminated, the mixing loss is significantly higher. The fact that the peak in the gap exit flow for the flat tipped blade is no longer present cannot explain the failure to validate the hypothesis. The flat tipped blade still has the lowest mixing loss and is virtually the same as when the peak was present.

It had been hoped to extend the measurements to cover the detailed flow on the endwall for each tip geometry before attempting to review the hypothesis or to attempt an explanation of why it was not validated. In the absence of these results it would appear that the interaction of the leakage jet with the main flow is much more complex than originally suggested and clearly a great deal more research is required in order to arrive at the reasons for any performance changes realised. The rapid growth of mixing loss over the last 20% of chord needs urgent explanation.

The mixing loss is also not simply a function of the leakage mass flow or of the gap discharge coefficient. Dishart and Moore (1989) found that the mixing loss was almost identical to the difference between the normal kinetic energy leaving the clearance gap and the secondary kinetic energy at cascade exit for a sharp edged square tipped blade. In each of the present cases the mixing loss was slightly lower than this kinetic energy difference, 78% for the square blade, 97% for the radiused blade and 80% for the contoured blade.

6 Exit Plane and Endwall Traverses.

The gradual development of the leakage vortex on the endwall from the 40% axial station where it is very small and close to the suction surface to the exit plane (100% axial) is shown in Figure 4 for the square tip. At all stations the leakage jet clings to the endwall and lifts off suddenly to roll into the vortex. Between the 80% and 90% stations, the distance of the center of the vortex from the suction surface almost doubles.

The vortex pattern in the exit plane for the contoured clearance gap shape is presented in Figure 5. The vortex center is further away from the blade and the secondary kinetic energy is the lowest of all three tip shapes which could partly contribute to the improved performance.

7 Simulated Rotor Performance.

When the total to static performances of the two new radiused tip shapes are compared with the original datum flat tipped sharp edged blade, the efficiency resulting from the simulated rotor analysis is 4.9% higher for the contoured tip and 3.7% lower for the blade with the simply radiused edge. Since the improvement with the contoured tip relates to the flow through a blade height of 1/4 chord, the improvement for a short blade of aspect ratio 1 would be approximately 1.2% and for a long blade with an aspect ratio of 2 it would be in the region of 0.6%.

The total to total efficiency is surprisingly different. The contoured tip has only a 1.2% improvement while the radiused edge is only 1.4% down. The reason for this is the significant difference in leaving kinetic energy (\bar{V}_2) for the two shapes, a factor that does not affect the total to total result.

While these results may be of some importance to designers of small machines which tend to have low aspect ratio blades ground sharply square at the tip for minimum clearance, of greater importance is that cascade data has been used to compare one rotor tip gap

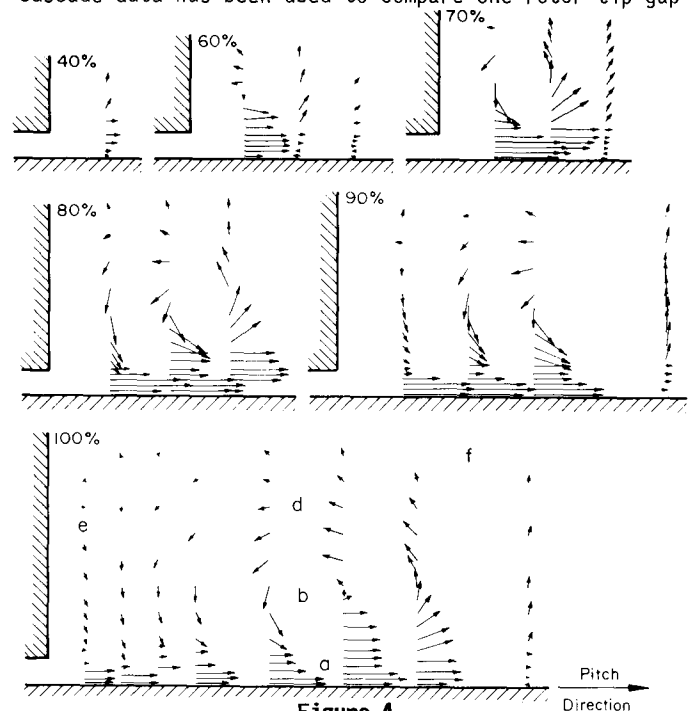


Figure 4 The development of the leakage vortex at various axial chord positions for square sharp edges tip.

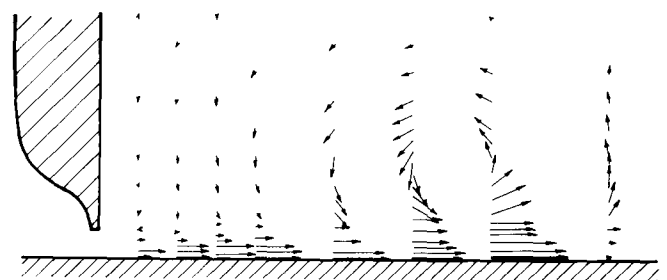


Figure 5 The exit plane (100% chord) leakage vortex for the contoured clearance gap.

geometry with another. A wide range of geometries pertinent to the type of turbine built can thus be compared before final testing and selection.

The relative rank in performance is also shown by the total pressure loss coefficient. Although it is logical, it is difficult to prove that the simulated rotor efficiency analysis method is a more reliable quantity. Rotor flows may well exist where pressure loss and efficiency show a contradictory performance rank of one geometry with respect to another.

Another significant result is that all three leakage flows have a much higher absolute outlet velocity than does the zero clearance case. To show this and to highlight the distortion caused to the exit velocity triangles by leakage and total pressure loss, Figure 6 presents diagrams at various points in the flow field for the square tipped blade and Figure 7 the averaged or mean result for each tip shape. The mean flow field diagrams show that tip clearance increases the axial velocity and decreases the deflection when compared to the zero clearance case which adversely affects work transfer and leaving loss. The most interesting vector plots are those in the vortex region. In the center of the vortex where there is high loss, Figure 6b shows that despite the high loss the "relative" velocity W_2 is as high as in the freestream due to the low static pressure in the middle of the rotating flow field. The work transfer is still good as reflected by the small exit swirl. At the top of the vortex (Figure 6d) there is an even better work transfer and swirl. At the bottom of the vortex (Figure 6a) which is in reality the low loss leakage jet flowing near the endwall, the swirl velocity is very large as is the axial velocity, both factors contributing to this segment of the flow field having a poor performance. Near the trailing edge wake (Figure 6e), the total pressure loss has reduced the "relative" velocity W_2 and the swirl is therefore high with a low work content.

The results in Table 1 are for W/U ratio of 0.5. Figure 8 shows the results over a range of blade speed ratios. The effect upon the total to static efficiency is minimal but the total to total efficiency increases with increasing blade speed. It would seem that at the higher blade speed, more work is extracted from the flow but at the penalty of an increased leaving loss, the latter fact not being reflected in the total to total concept.

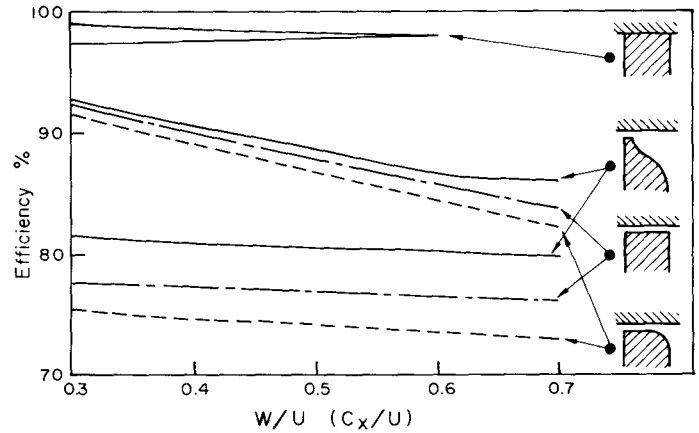


Figure 8
Total to total efficiency (upper curves)
Total to static efficiency (lower curves)
over a range of blade speed W/U (C_x/U) ratios

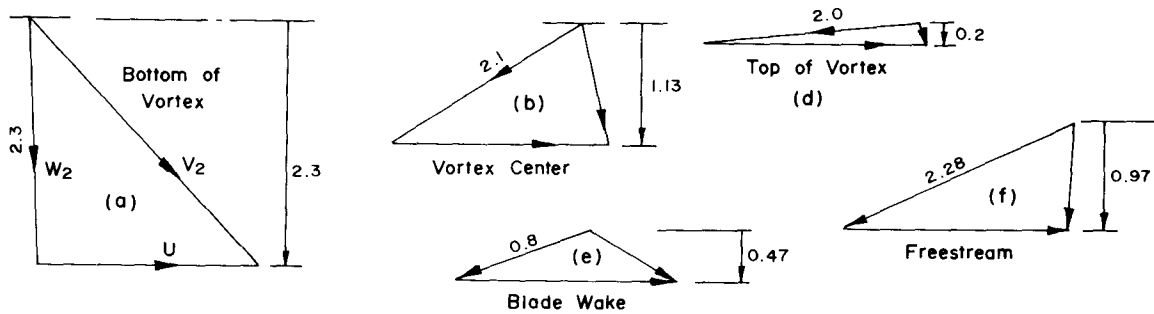


Figure 6
Velocity triangles at various points marked in the exit plane flow field in Figure 4 of the square sharp edged blade showing the influence of flow phenomena on exit swirl and local work transfer.

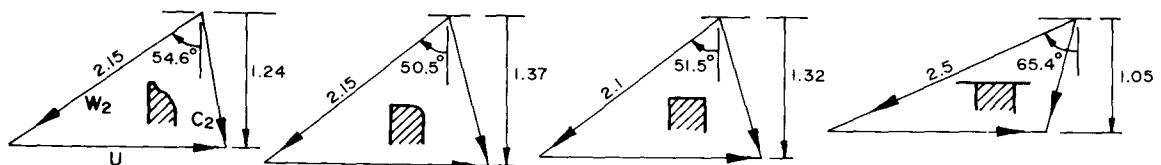


Figure 7
Mean flow field outlet velocity triangles for zero clearance and for the three tip gap shapes.

8 Conclusions

It was shown that radiusing and contouring the leakage gap geometry to prevent the formation of the separation bubble significantly reduced the internal gap loss which had been shown to form from 35% to 38% of the overall cascade total pressure deficit.

The relationship between the bubble and the leakage mixing loss was not established. The two geometries that avoided bubble formation both showed a higher mixing loss. However the leakage jet entering the flow did not show the high loss concentration that had previously been associated with the separation bubble.

A method whereby detailed stationary cascade flow field data can be converted into a simulated rotor flow to calculate work transfer and efficiency was presented and its use demonstrated by comparing the endwall region performance of the the tip clearance geometries tested. The contoured tip with a loss free gap flow and reduced leakage rate by radial deflection of the jet showed a better performance than the datum sharp edged square tip despite having almost the same overall loss coefficient. These results show the usefulness of the method and points the way towards using stationary cascades to develop tip geometries for better performance.

The improved tip geometry realised in this paper was primarily studied in order to reveal fundamental flow phenomena changes. In practice the increase in efficiency would be applicable only to sharply ground flat tipped blades and would depend on the length of the blade and on what type of efficiency is quoted. Nevertheless, the fact that the internal gap loss has been greatly reduced and the fact an improved performance was achieved is regarded as encouraging.

The results of this paper seem to indicate that tip clearance flow and loss is very sensitive to geometry and flow conditions. The internal gap loss measured for the square edged blade was not the same as previously measured and the high loss wake in the gap exit flow was not reproduced. Further study is warranted to test new shapes for loss reduction and for the purpose of understanding the factors involved in determining rotor efficiency.

BIBLIOGRAPHY

Bindon J P, 1987, "The measurement of tip clearance flow structure on the endwall and within the clearance gap of an axial turbine cascade" Proc. I Mech. E. Int Conference Turbomachinery-Efficiency Prediction and Improvement, Cambridge, paper C273/87

Bindon J P, 1988, "The measurement and formation of tip clearance loss", ASME Paper 88-GT-203, Transactions of ASME, J of Turbomachinery, V 111, N 3, July 1989, p 257

Booth T C, Dodge P R, Hepworth H K, 1982 "Rotor tip leakage: Part 1-Basic Methodology" ASME Transactions, J of Engineering for Power, V 104, Jan 1982, p 154

Dishart P T, Moore K, 1989 "Tip leakage losses in a linear turbine cascade" ASME Paper 89-GT-56

Morphis G, Bindon J P, 1988, "The effects of relative motion, blade edge radius and gap size on the blade tip pressure distribution in an annular turbine with tip clearance", ASME Paper 88-GT-256.

Offenberg L, Fischer J, Vander Hoek T, 1987 "An experimental investigation of turbine case treatments", 23rd AIAA/SAE/ASME/ASEE Joint Propulsion Conference, San Diego, June 29 1987.